Mg-induced increase of bandgap in $Zn_{1-x}Mg_xO$ nanorods revealed by x-ray absorption and emission spectroscopy

J. W. Chiou [a)]
Department of Applied Physics, National University of Kaohsiung, Kaohsiung 811, Taiwan
H. M. Tsai, C. W. Pao, F. Z. Chien and W. F. Pong [b)]
Department of Physics, Tamkang University, Tamsui 251, Taiwan
C. W. Chen
Department of Materials Science and Engineering, National Taiwan University, Taipei 106, Taiwan
M.-H. Tsai
Department of Physics, National Sun Yat-Sen University, Kaohsiung 804, Taiwan
J. J. Wu, C. H. Ko and H. H. Chiang
Department of Chemical Engineering, National Cheng Kung University, Tainan 701, Taiwan
H.-J. Lin and J. F. Lee
National Synchrotron Radiation Research Center, Hsinchu 300, Taiwan
J.-H. Guo
Advanced Light Source, Lawrence Berkeley National Laboratory, Berkeley, CA 94720

Abstract

X-ray absorption near-edge structure (XANES) and x-ray emission spectroscopy (XES) measurements were used to investigate the effect of Mg doping in ZnO nanorods. The intensities of the features in the O *K*-edge XANES spectra of $Zn_{1-x}Mg_xO$ nanorods are lower than those of pure ZnO nanorods, suggesting that Mg doping increases the negative effective charge of O ions. XES and XANES spectra of O 2*p* states indicate that Mg doping raises (lowers) the conduction-band-minimum (valence-band-maximum) and increases the bandgap. The bandgap is found to increase linearly with the Mg content, as revealed by photoluminescence and combined XANES and XES measurements.

PACS Number: 78.70.Dm; 73.63.-b; 61.46.-w

1. Introduction

The wide bandgap II-VI semiconductor alloy, ZnMgO, has attracted extensive interest in recent years because of its fundamental and technological importance in ZnMgO/ZnO-based superlattice structures.[1-3] The photoluminescence (PL) measurements of Mg doped ZnO nanowires/nanorods revealed a blueshift in near-band-edge (NBE) emission as the Mg content is increased,[4-6] suggesting that this material may be suitable for use in tunable electronic and optical nanodevices. Raman spectra indicated that the disorder associated with the incorporation of Mg dopants enhanced exciton localization and asymmetrically broadened the phonon line-shapes of $Zn_{1-x}Mg_xO$ nanocrystals.[7] The extended x-ray absorption fine structure (EXAFS) also demonstrated that the blueshift of the bandgap (E_g) of $Zn_{1-x}Mg_xO$ thin films was associated with the increase of the structural distortion/disorder.[8] Although PL measurements have revealed the blueshift in E_g in the $Zn_{1-x}Mg_xO$ alloys, the engineering of E_g by altering the electronic density of states (DOSs) at/near conduction-band-minimum (CBM) and valence-band-maximum (VBM) by doping Mg to ZnO nanomaterials has not been extensively investigated.[9-11] Knowledge of the dependence of the electronic structures of $Zn_{1-x}Mg_xO$ nanomaterials on Mg doping is crucial to understanding the basic physics that underlie their nanotechnological applications. Chang *et al*. attempted to elucidate the correlation between the electronic structures and the optical properties of $Zn_{1-x}Mg_xO$ nanorods.[10] Here, a combination of PL, EXAFS, x-ray absorption near-edge structure (XANES) and x-ray emission spectroscopy (XES) was used to investigate the increase of E_g by the doping of Mg in ZnO nanorods.

2. Experimental details

O and Mg *K*-edge, Zn L_3-edge XANES and Zn *K*-edge EXAFS spectra were obtained in the fluorescence mode, using the high-energy spherical grating monochromator-20A, Dragon-11A and wiggler-17C beamlines, respectively, at the National Synchrotron Radiation Research Center in Hsinchu, Taiwan. The XES and corresponding XANES measurements at the O *K*-edge were carried out at beamline-7.0.1 at the Advanced Light Source, Lawrence Berkeley National Laboratory. The angle of incidence of the incoming photon with respected to the normal direction of the sample's surface was approximately 37^0. The resolutions were set to 0.1-0.2eV at a photon energy of 530-1300eV during XANES measurements, while the resolution of the XES measurement was set to ~0.35eV. The well-aligned $Zn_{1-x}Mg_xO$ (x= 0, 0.03, 0.07, 0.10 and 0.12) nanorods were prepared on the Si(100) substrate using catalyst-free metalorganic chemical vapor deposition. Room-temperature PL spectra were obtained using the emission of the Xe lamp with a wavelength of 325nm. The size of $Zn_{1-x}Mg_xO$ nanorods was measured using high-resolution transmission electron microscopy (HR-TEM). The nanorods had a diameter of ~50±10 nm and a length of ~450±10 nm. Heo *et al*. reported that due the limited solubility of Mg in ZnO, ZnMgO nanostructures may grow in a core-shell structure with a low Mg core surrounded by a shell with a higher Mg content.[12] Therefore, $Zn_{1-x}Mg_xO$ nanorods were also characterized using HR-TEM. Analyses of the bottom, middle and top regions of the nanorods show an absence of segregated structures of the impurity phase, indicating that $Zn_{1-x}Mg_xO$ nanorods have mainly a single-phase structure. Details of the preparation and characterization of $Zn_{1-x}Mg_xO$ nanorods have been presented elsewhere.[5]

3. Results and discussion

The inset (a) in Fig. 1 presents the scanning electron microscopic (SEM) image of $Zn_{0.97}Mg_{0.03}O$ nanorods. X-ray diffraction (XRD) patterns in inset (b) reveal that the doping of Mg does not change the wurtzite structure of host ZnO nanorods. $Zn_{1-x}Mg_xO$ nanorods show a predominant (002) reflection at ~34.5^0, indicating that the nanorods are preferentially oriented along the ***c***-axis. Evidently, the XRD spectra of the $Zn_{1-x}Mg_xO$ nanorods do not exhibit any Bragg peak of MgO or Mg metal, further supporting the HR-TEM observation that $Zn_{1-x}Mg_xO$ nanorods have mainly a single-phase structure, without MgO phase segregation or the formation of a Mg core-shell structure in $Zn_{1-x}Mg_xO$ nanorods, as proposed by Heo *et al*.[12] Inset (c) shows the NBE emission in the PL spectra of $Zn_{1-x}Mg_xO$ nanorods, clearly indicating that the shifts of the PL-maximum position from ~3.3 (x= 0) to 3.5 eV (x= 0.12). This blueshift in the NBE emission cannot be caused by the quantum confinement effect, because the sizes of the $Zn_{1-x}Mg_xO$ nanorods in all of the samples are almost the same and are far beyond the quantum confinement regime. Figure 1 also presents the Fourier transform (FT) of EXAFS $k^3\chi$ data at the Zn *K*-edge. The general line-shapes and radial distribution of the FT spectra of $Zn_{1-x}Mg_xO$ nanorods are similar to those of pure ZnO nanorods, suggesting Mg is substituted at the Zn sites. The first two main peaks in the FT spectra correspond to the nearest-neighbor Zn-O and the next-nearest-neighbor Zn-Zn/Zn-Mg bond lengths,[8] respectively. Their overall intensities decrease as the Mg content in the $Zn_{1-x}Mg_xO$ nanorods increases, which can be due to the increase of the structural disorder/distortion at the Zn sites in the $Zn_{1-x}Mg_xO$ nanorods. Park *et al*. observed a similar trend for $Zn_{1-x}Mg_xO$ thin films.[8]

Figure 2(a) presents the normalized O *K*-edge XANES spectra of $Zn_{1-x}Mg_xO$ nanorods. Features A_1-E_1 of $Zn_{1-x}Mg_xO$ nanorods are attributable to electron transitions from O 1*s* to unoccupied O $2p_\pi$ (along the ***c***-axis) and O $2p_\sigma$ (in the bi-layer) states.[9,13,14] The line-shapes of the O *K*-edge XANES spectra of $Zn_{1-x}Mg_xO$ nanorods are very similar to those of ZnO nanorods (x= 0). However, the overall intensities of the features of $Zn_{1-x}Mg_xO$ nanorods are lower than those of ZnO nanorods, reflecting the reduction in the number of unoccupied O 2*p*-derived states. The decrease in the O *K*-edge XANES intensity suggests an increase in the occupation of the O 2*p*-orbitals or the number of electrons in O ions. The increase in the number of electrons in O ions by Mg doping is understandable, because Mg has a significantly smaller electronegativity (1.31) than that of Zn (1.65),[15] such that more electrons are transferred from Mg to the O 2*p* states, and the ionic character of the $Zn_{1-x}Mg_xO$ alloys is increased.[10,11] Previous studies of $Zn_{1-x}Co_xO$ nanorods indicated that the intensity of the O *K*-edge XANES feature decreases as the Co content increases,[9] despite the fact that Co has an electronegativity that is larger than that of Zn. This can be understood by the fact that Co has additional 3*d* states, which are absent from Mg. The decrease in intensity due to Co doping can be interpreted as being caused by O 2*p*-Co 3*d* hybridization, which lowers the energies of O 2*p* orbitals, enhancing the occupation of O 2*p* orbitals. The higher O 2*p* occupation associated with smaller electronegativity of Mg is consistent with the higher the intensity of the valence-band photoemission spectra in Fig. 4 of Ref. 9. The inset in Fig. 2(a) shows that the threshold in the O *K*-edge XANES spectra moves slightly toward higher energy as the Mg content in the $Zn_{1-x}Mg_xO$ nanorods increases. Figure 2(b) presents the normalized Mg *K*-edge XANES spectra of $Zn_{1-x}Mg_xO$. The partial DOSs calculated using the CASTEP code,[16] based on the

plane-wave pseudopotential method with the local density approximation for $Zn_{1-x}Mg_xO$,[10] indicates that the three main features, **A_2-C_2**, are associated primarily with Mg 3*p*-O 2*p* hybridized states. The intensities of features **A_2-C_2** clearly increase with the Mg content, suggesting that the increase in the number of unoccupied Mg 3*p*-derived states is associated with the transfer of electrons from Mg to O atoms as the Mg content increases, in a manner consistent with the O *K*-edge XANES measurements. The inset in Fig. 2(b) also presents the normalized Zn L_3-edge XANES spectra of $Zn_{1-x}Mg_xO$ nanorods, which reveal electron transitions from Zn 2*p* states to unoccupied Zn 4*sd* states.[9,13,17] Figure 2(b) shows that the unoccupied Zn 4*sd* states are insensitive to Mg doping. Indeed, the calculated unoccupied partial DOSs of Zn 4*s* states in Ref. 10 for $Zn_{1-x}Mg_xO$ are similar to that for ZnO.

Figure 3 displays XES and corresponding XANES spectra of O 2*p* states of $Zn_{1-x}Mg_xO$ nanorods. The maximum intensities of the features in the XES and XANES spectra were arbitrarily normalized to unity. The O K_α-emission spectra reflect O 2*p* occupied (valence-band) states and O *K*-edge XANES spectra reflect O 2*p* unoccupied (conduction-band) states of $Zn_{1-x}Mg_xO$ nanorods. The spectra in Fig. 3 are similar to those of ZnO nanoparticles reported elsewhere.[18] A well-defined bandgap, E_g, indicated by the dotted lines is obtained by extrapolating the leading edges in the XANES and XES spectra to the baselines, which correspond to the CBM and VBM,[18,19] respectively. Apparently, the threshold in the O *K*-edge XANES (O K_α XES) spectra overall moves slightly toward higher (lower) energy as the Mg content is increased, as can be seen on the magnified scale in inset (a) [inset (b)]. This result is consistent with the measurements shown in Fig. 2(a). Nevertheless, the combined emission and absorption spectra demonstrate that E_g is ~3.3eV for pure ZnO nanorods and systematically increases

with the Mg content in the $Zn_{1-x}Mg_xO$ nanorods, as plotted in inset (c). These results are consistent with the general trend of NBE emission that was revealed by PL measurements [data obtained from inset (c) in Fig. 1]. The E_g values that were determined from the combined XES and XANES measurements were slightly larger than those determined from the NBE emission data. Since NBE emission is the result of free exciton emission,[10] the difference between E_g values and emission data, ΔE_g, can be attributed to the difference between the energy of CBM and the exciton level, which is approximately tens of meV in $Zn_{1-x}Mg_xO$ nanorods. The ΔE_g of ~40meV for x= 12%, is the largest for any $Zn_{1-x}Mg_xO$ nanorods. Recently, temperature-dependent PL studies have found that the exciton was bound by an energy of 50-60meV (depending on Mg doping) in $Zn_{1-x}Mg_xO$ nanorods,[20] suggesting that ΔE_g ~50-60 meV. The discrepancy may be due to the limited of the energy resolutions of the XES and XANES measurements ~0.35eV and 0.1eV respectively.

Several factors are believed to affect the shifts of NBE emission in the PL spectra of $Zn_{1-x}Mg_xO$ alloys upon the doping of ZnO with Mg. Excitonic transitions (exciton-related recombination), alloy-induced structural disorder/distortion effects, quantum confinement, surface effects/defects and bulk defects, such as oxygen vacancies, are present.[6-8,21,22] The FT analysis of EXAFS results suggests Mg-induced structural disorder/distortion at the Zn sites in $Zn_{1-x}Mg_xO$ nanorods. Structural disorder/distortion typically is responsible for potential fluctuation in the alloy, enhancing excitonic transition.[7] This phenomenon may be related to native defects in the ZnMgO alloy, since Mg doping shifts CBM toward higher energy, away from the intrinsic shallow donor states, and increases the activation energy of defect donors, increasing the emission-energy in the PL spectra.[23,24] Importantly,

combining O K_α XES and the corresponding O *K*-edge XANES spectra in Fig. 3 demonstrates that the increase in E_g, is associated with the shifts in CBM (VBM) toward higher (lower) energy upon the doping of host ZnO nanorods with Mg. Previous theoretical calculations have indicated that the widths of both O 2*p* and Zn 3*d* bands become narrower and their partial DOSs near the top of valence bands increase with the increase of x in $Zn_{1-x}Mg_xO$,[10] suggesting that Mg-induced enhancement of the localization of O 2*p* and Zn 3*d* states as well as the ionic character of $Zn_{1-x}Mg_xO$. As a result, the screening effect is reduced and the exciton energy is increased, which may explain the linear increase of ΔE_g in the inset of Fig. 3.

4. Conclusion

O *K*-edge XANES measurements suggest that Mg doping increased the negative effective charge of oxygen ions. O *K*-edge XES and XANES spectra demonstrate that Mg doping raises and lowers conduction- and valence-band edges, respectively, thus increasing E_g. Both PL and combined XES and XANES measurements show that E_g increases linearly with Mg content.

Acknowledgements

The author (WFP) would like to thank the National Science Council of Taiwan for financially supporting this research under Contract No. NSC96-2112-M032-012-MY3. The Advanced Light Source is supported by the Director, Office of Science, Office of Basic Energy Sciences, of the U.S. Department of Energy under Contract No. DE-AC02-05CH11231.

[a)] Electronic mail: jwchiou@nuk.edu.tw

[b)] On leave at Advanced Light Source, LBNL, Berkeley, CA

References

[1] A. Tsukazaki, A. Ohtomo, T. Kita, Y. Ohno, H. Ohno, and M. Kawasaki, Science **315**, 1388 (2007).

[2] V. A. Fonoberov and A. A. Balandin, J. Phys.: Condens. Matter **17**, 1085 (2005).

[3] A. Malashevich and D. Vanderbilt, Phys. Rev. B **75**, 045106 (2007).

[4] T. Makino, Y. Segawa, M. Kawasaki, A. Ohtomo, R. Shiroki, K. Tamura, T. Yasuda, and H. Koinuma, Appl. Phys. Lett. **78**, 1237 (2001).

[5] C. H. Ku, H. H. Chiang, and J. J. Wu, Chem. Phys. Lett. **404**, 132 (2005).

[6] H. C. Hsu, C. Y. Wu, H. M. Cheng, and W. F. Hsieh, Appl. Phys. Lett. **89**, 013101 (2006).

[7] J. D. Ye, K. W. Teoh, X. W. Sun, G.. Q. Lo, D. L. Kwong, H. Zhao, S. L. Gu, R. Zhang, Y. D. Zheng, S. A. Oh, X. H. Zhang, and S. Tripathy, Appl. Phys. Lett. **91**, 091901 (2007).

[8] S.-H. Park, K.-B. Kim, S.-Y. Seo, S.-H. Kim, and S.-W. Han, J. Electronic Materials **35**, 1680 (2006).

[9] J. W. Chiou, H. M. Tsai, C. W. Pao, K. P. Krishna Kumar, S. C. Ray, F. Z. Chien, W. F. Pong, M.-H. Tsai, C.-H. Chen, H.-J. Lin, J. J. Wu, M.-H. Yang, S. C. Liu, H. H. Chiang, and C. W. Chen, Appl. Phys. Lett. **89**, 043121 (2006).

[10] Y. S. Chang, C. T. Chien, C. W. Chen, T. Y. Chu, H. H. Chiang, C. H. Ku, J. J. Wu, C. S. Lin, L. C. Chen, and K. H. Chen, J. Appl. Phys. **101**, 033502 (2007).

[11] M. K. Yadav, M. Ghosh, R. Biswas, A. K. Raychaudhuri, A. Mookerjee, and S. Datta, Phys. Rev. B **76**, 195450 (2007).

[12] Y. W. Heo, D. P. Norton, L. C. Tien, Y. Kwon, B. S. Kang, F. Ren, S. J. Pearton, and J. R. LaRoche, Mat. Sci, Eng. R **47**, 1 (2004).

[13] J. W. Chiou, K. P. Krishna Kumar, J. C. Jan, H. M. Tsai, C. W. Bao, W. F. Pong, F. Z. Chien, M.-H. Tsai, I.-H. Hong, R. Klauser, J. F. Lee, J. J. Wu, and S. C. Liu, Appl. Phys. Lett. **85**, 3220 (2004).

[14] J. W. Chiou, J. C. Jan, H. M. Tsai, C. W. Bao, W. F. Pong, M.-H. Tsai, I.-H. Hong, R. Klauser, J. F. Lee, J. J. Wu, and S. C. Liu, Appl. Phys. Lett. **84**, 3462 (2004).

[15] *Table of periodic properties of the elements*, Sargent-Welch Scientific Company, Skokie, Illinois (1980).

[16] T. Mizoguchi, A. Seko, M. Yoshiya, H. Yoshida, T. Yoshida, W. Y. Ching, and I. Tanaka, Phys. Rev. B **76**, 195125 (2007).

[17] M. C. Payne, M. P. Teter, D. C. Allan, T. A. Arias, and J. D. Joannopoulos, Rev. Mod. Phys. **64**, 1045 (1992).

[18] C. L. Dong, C. Persson, L. Vayssieres, A. Augustsson, T. Schmitt, M. Mattesini, R. Ahuja, C. L. Chang, and J.-H. Guo, Phy. Rev. B **70**, 195325 (2004).

[19] J. W. Chiou, S. C. Ray, H. M. Tsai, C. W. Pao, F. Z. Chien, W. F. Pong, M-H. Tsai, J. J. Wu, C. H. Tseng, C.-H. Chen, J. F. Lee, and J.-H. Guo, Appl. Phys. Lett. **90**, 192112 (2007).

[20] J. G. Lu, Y. Z. Zhang, Z. Z. Ye, Y. J. Zeng, J. Y. Huang, and L. Wang, Appl. Phys. Lett. **91**, 193108 (2007).

[21] Ü. Özgür, Ya. I Alivov, C. Liu, A. Teke, M. A. Reshchikov, S. Doğan, V. Avrutin, S.-J. Cho, and H. Morkoç, J. Appl. Phys. **98**, 041301 (2005).

[22] V. A. Fonoberov and A. A. Balandin, J. Nanoelectronics and Optoelectronics **1**, 19 (2006).

[23] Y. W. Heo, Y. W. Kwon, Y. Li, S. J. Pearton, and D. P. Norton, Appl. Phys. Lett. **84**, 3474 (2004).

[24] Y. J. Zeng, Z. Z. Ye, Y. F. Lu, J. G. Lu, L. Sun, W. Z. Xu, L. P. Zhu, B. H. Zhao, and Y. Che, Appl. Phys. Lett. **90**, 012111 (2007).

Figure Captions

Fig.1 Magnitude of FT of EXAFS $k^3\chi$ data at the Zn *K*-edge of $Zn_{1-x}Mg_xO$ nanorods. Insets (a)-(c) present, SEM image (x= 0.03), XRD patterns and PL spectra of $Zn_{1-x}Mg_xO$ nanorods, respectively.

Fig. 2(a) Normalized O *K*-edge XANES spectra of $Zn_{1-x}Mg_xO$ nanorods. The inset shows a magnified view of edge features of O *K*-edge XANES spectra. (b) Normalized Mg *K*-edge XANES spectra of $Zn_{1-x}Mg_xO$ nanorods. The inset presents normalized Zn L_3-edge spectra of $Zn_{1-x}Mg_xO$ nanorods.

Fig. 3 XES and corresponding XANES of O 2*p* states of $Zn_{1-x}Mg_xO$ nanorods. Insets (a) and (b) show magnified views of edge features of O *K*-edge XANES and O K_α XES spectra, respectively. Inset (c) plots E_g and NBE emission data [inset (c) in Fig. 1] for various Mg content.

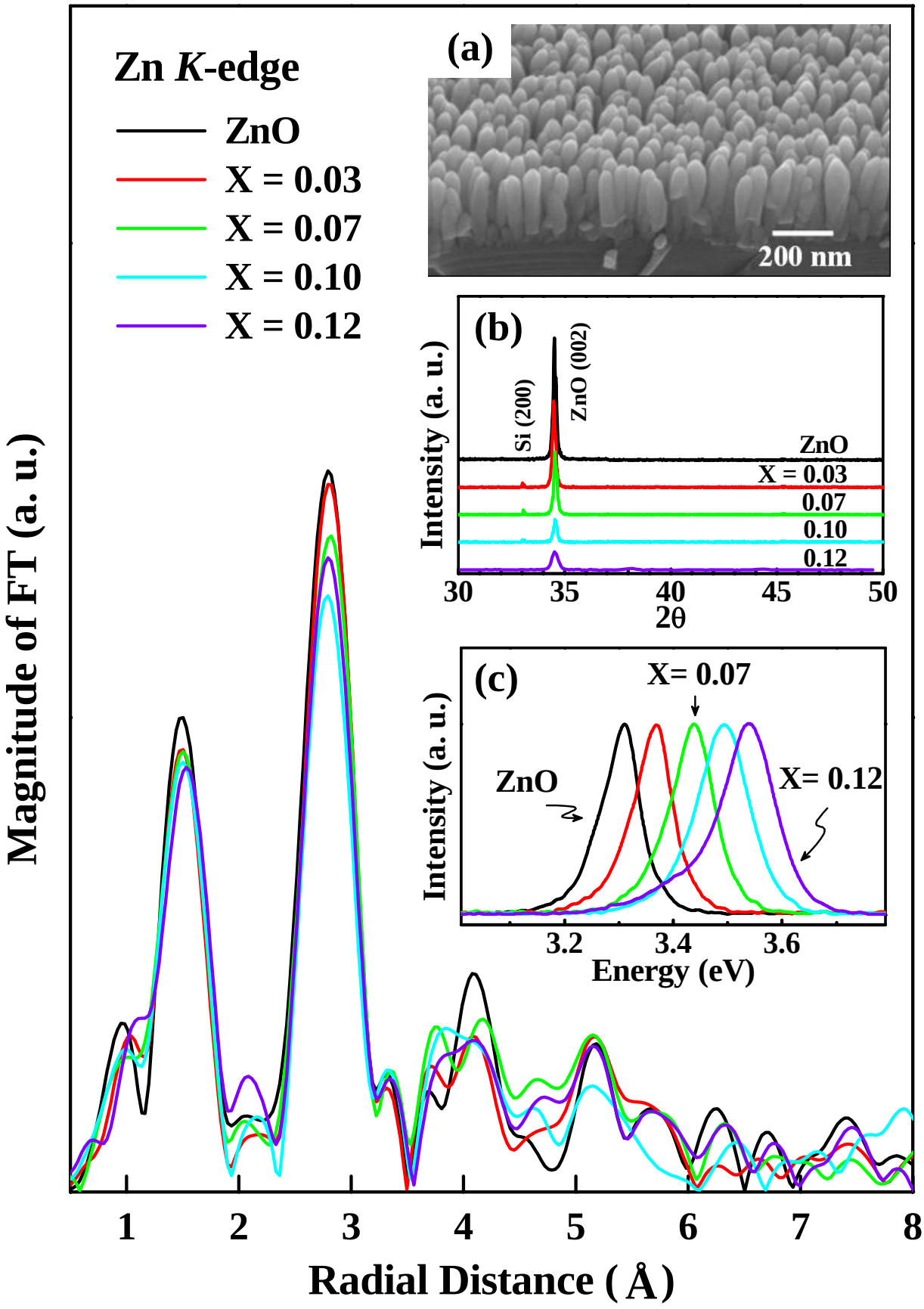
Zn K-edge
ZnO
X = 0.03
X = 0.07
X = 0.10
X = 0.12
(a)
200 nm
(b)
Si (200)
ZnO (002)
Intensity (a. u.)
ZnO
X = 0.03
0.07
0.10
0.12
30
35
40
45
50
2θ
(c)
X= 0.07
ZnO
X= 0.12
Intensity (a. u.)
3.2
3.4
3.6
Energy (eV)
Magnitude of FT (a. u.)
1
2
3
4
5
6
7
8
Radial Distance (Å)

Fig. 1

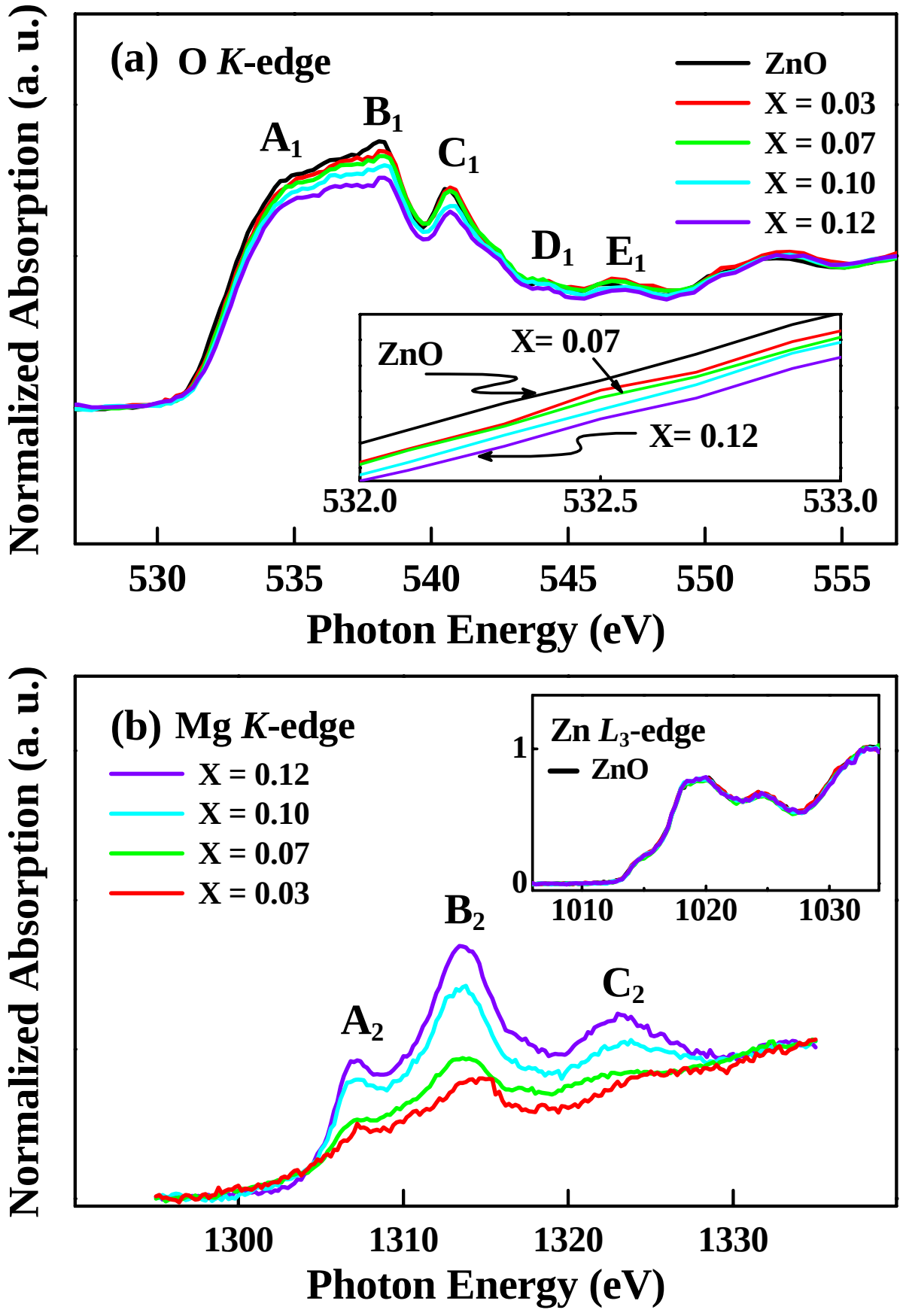
(a) O K-edge
ZnO
X = 0.03
X = 0.07
X = 0.10
X = 0.12
A1
B1
C1
D1
E1
ZnO
X= 0.07
X= 0.12
532.0
532.5
533.0
Normalized Absorption (a. u.)
530
535
540
545
550
555
Photon Energy (eV)
(b) Mg K-edge
X = 0.12
X = 0.10
X = 0.07
X = 0.03
Zn L3-edge
ZnO
1
0
1010
1020
1030
B2
C2
A2
Normalized Absorption (a. u.)
1300
1310
1320
1330
Photon Energy (eV)

Fig. 2

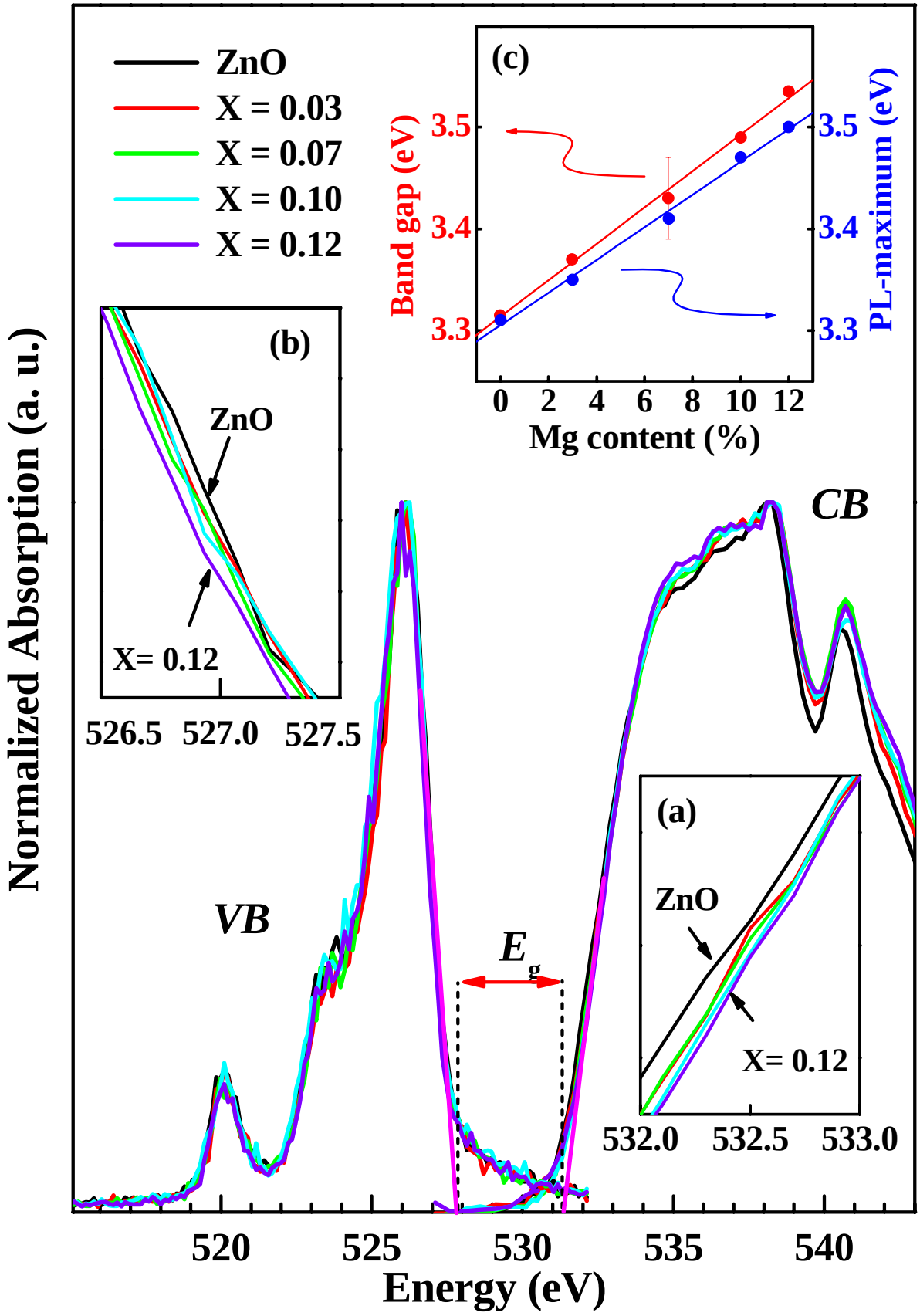
ZnO
X = 0.03
X = 0.07
X = 0.10
X = 0.12
(c)
Band gap (eV)
PL-maximum (eV)
3.5
3.4
3.3
0 2 4 6 8 10 12
Mg content (%)
(b)
ZnO
X= 0.12
526.5 527.0 527.5
CB
VB
E_g
(a)
ZnO
X= 0.12
532.0 532.5 533.0
Normalized Absorption (a. u.)
520 525 530 535 540
Energy (eV)

Fig. 3